In Situ Optical Absorption Mercury Continuous Emission Monitor

ARTICLE · DECEMBER 2009

DOI: 10.1021/es902409t · Source: PubMed

6 AUTHORS, INCLUDING:

Reza Mani
York University
10 PUBLICATIONS **50** CITATIONS
SEE PROFILE

William Morrow
Resonance Ltd.
13 PUBLICATIONS **92** CITATIONS
SEE PROFILE

Eric Morris
University of Toronto
7 PUBLICATIONS **46** CITATIONS
SEE PROFILE

Charles Q Jia
University of Toronto
80 PUBLICATIONS **803** CITATIONS
SEE PROFILE

In Situ Optical Absorption Mercury Continuous Emission Monitor

JÉRÔME THIEBAUD,[†,§] MURRAY J. THOMSON,[*,†] REZA MANI,[‡] WILLIAM H. MORROW,[‡] ERIC A. MORRIS,[¶] AND CHARLES Q. JIA[¶]

Department of Mechanical and Industrial Engineering, University of Toronto, 5 King's College Road, Toronto, ON, Canada M5S 3G8, Resonance Ltd., 143 Ferndale Drive North, Barrie, ON, Canada L4N 9 V9, and Department of Chemical Engineering and Applied Chemistry, University of Toronto, 200 College Street, Toronto, ON, Canada M5S 3E5

Received August 7, 2009. Revised manuscript received October 26, 2009. Accepted November 4, 2009.

This paper reports the development of an in situ continuous emission monitor (CEM) for measuring elemental mercury (Hg^0) concentration in the exhaust stream of coal-fired power plants. The instrument is based on the ultraviolet atomic absorption of a mercury lamp emission line by elemental mercury and a light-emitting diode (LED) background correction system. This approach allows an in situ measurement since the absorption of other species such as SO_2 can be removed to monitor the Hg^0 contribution only. Proof of concept was established through a laboratory-based investigation, and a limit of detection, $[Hg^0]_{min}$, of 2 $\mu g/m^3$ was measured for a 1-min averaged sample and an absorption path length of 49 cm. $[Hg^0]_{min}$ is anticipated to be better than 0.2 $\mu g/m^3$ across a 7 m diameter stack. Finally, the apparatus was field-tested in a 230 MW coal-fired power plant. The operability of the measurement in real conditions was demonstrated, leading to the first Hg^0 concentration values recorded by the in situ CEM. Comparison with an accepted standard method is required for validation.

Introduction

Mercury (Hg) is a health and ecological concern because of its toxic, persistent, and bioaccumulative properties. The major anthropogenic source of both elemental (Hg^0) and oxidized Hg arises from coal-based power generation. Once released to the environment, it is converted by the action of anaerobic organisms that live in aquatic systems to the highly toxic form, methylmercury, which accumulates in fish and other aquatic species (*1*). In 2006, Canada-wide Standards mandated that 60% of mercury emissions would be captured by 2010 and possibly 80% by 2018 (*2*). In the United States, the EPA's Clean Air Mercury Rule creates a market-based cap-and-trade program that will reduce nationwide utility emissions of mercury (*3*). In anticipation of these regulations, there has been much research carried out in developing new mercury capture technologies (*4, 5*). New sensors are also needed to assess the efficiency of these removal strategies as well as the compliance of coal combustors with emissions regulations. Indeed, the currently accepted standard for monitoring Hg in coal-fired utility exhaust relies on wet-chemistry methods: these are slow, expensive, and require highly trained personnel (*6*). Alternatively, optical techniques have been developed to provide real-time measurements of mercury, which can be sorted into two categories: extractive and in situ techniques. The extractive systems are the most common and are commercially available. They consist of a sampling unit, a probe located in the exhaust flue, a pretreatment unit to remove all interfering species and particulates, and an analytical unit. To determine the concentration of mercury present in the sample, an ultraviolet lamp is used to perform either absorption or fluorescence spectroscopy. The pretreatment step is required to remove interfering species such as SO_2, which absorb at the same wavelength as Hg^0, or to preconcentrate the sample to improve the detection limit. However, the extractive approach has limitations: the probe may get clogged; heterogeneous reactions and adsorption may occur in the sampling line; and delays because of sample travel and treatment are inherent.

To overcome these issues, nonintrusive approaches (measuring Hg directly in the flue gas) have been developed. In the late 1990s, laser induced break-down spectroscopy (LIBS) appeared to be a promising technique for an in situ Hg CEM. By creating a laser spark in the probe volume, excited mercury atoms emit light at their 253.7 nm specific wavelength. This atomic emission technique is advantageous since it can detect many species simultaneously, independently of their initial form. This is possible because the plasma is hot enough to dissociate molecules such as mercuric chloride into their constituent atoms, and thus total mercury is measured. Furthermore, only one optical port is necessary since the laser pulse can use the same window as the collecting optics. However, the calibration of such an instrument is very difficult because the atomic emission is affected by quenching due to other species in the gaseous medium (*7*). In addition, the minimum detectable Hg concentration reached with this approach (80 $\mu g/m^3$ (*8*)) is not low enough for monitoring mercury emitted by coal-fired power plants which is typically present in concentrations between 1 and 30 $\mu g/m^3$ (*9, 10*).

Better sensitivity can be achieved using atomic absorption of Hg^0 at 253.7 nm: the strong absorption cross-section at this wavelength combined with an absorption path length longer than 50 cm can lead to a suitable sensitivity for monitoring mercury in coal-fired utilities. It must be mentioned that, unlike LIBS, only the atomic form of mercury, Hg^0, is detected by this approach. However, oxidized and particle-bound forms of mercury are efficiently removed by air pollution control devices from the exhaust gas: oxidized mercury is soluble associates easily with particles, and is filtered out by devices, such as fabric filters and electrostatic precipitators (*11, 12*). Conversely, atomic mercury is difficult to capture because it is volatile and insoluble, and this strengthens the need of efficient CEM able to quantify it in real time.

As several species present in the coal combustion exhaust absorb around 254 nm, an in situ measurement must discriminate the contribution of Hg^0 from the signal given by interfering species such as SO_2. A recent breakthrough in diode laser frequency-mixing has been shown to overcome this issue by providing a UV continuous-wave laser output (*13, 14*). The laser radiation, quasi-monochromatic compared

* Corresponding author e-mail: thomson@mie.utoronto.ca.
† Department of Mechanical and Industrial Engineering, University of Toronto.
‡ Resonance Ltd.
¶ Department of Chemical Engineering and Applied Chemistry, University of Toronto.
§ Current address: SRI International, 333 Ravenswood Avenue, Menlo Park, CA 94025.

10.1021/es902409t

Published on Web 11/19/2009

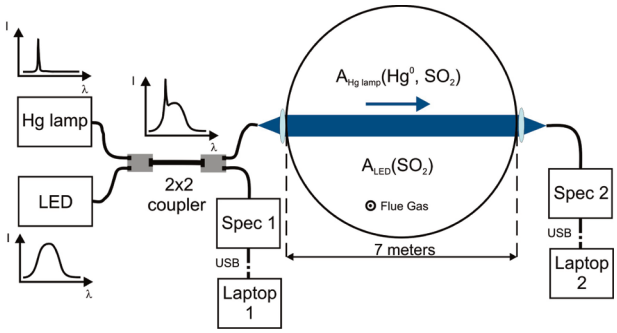

FIGURE 1. Top-view schematic of the instrumental setup.

to the Hg^0 absorption line, enables one to spectrally resolve the Hg^0 feature and thus distinguish it from the broad background caused by interfering absorption and light scattering. Although a sub-parts-per-billion limit of detection has been demonstrated, this expensive system remains experimentally challenging and is thus poorly suited to run continuously in a harsh industrial environment. Furthermore, it delivers a weak optical power (a few μW) which becomes an issue in the presence of large scattering or absorption.

The instrument presented in this paper is also based on ultraviolet atomic absorption of mercury and achieves a suitable level of selectivity and sensitivity with inexpensive components. The Hg^0 CEM and its ability to perform in a practical setting was demonstrated during a field campaign at a 230 MW coal-fired power plant. This sensor shows great promise as a tool for assessing mercury-capture strategies as well as the compliance of coal-fired utilities with environmental regulations.

Method and Instrumental Apparatus

The sensor makes use of the absorption of elemental mercury at 253.7 nm to determine its concentration in the gaseous exhaust of coal-fired utilities. For this purpose, an electrodeless radio frequency excited mercury lamp, which exhibits a strong emission line at 253.7 nm, was used for monitoring the light attenuation at this wavelength. However, sulfur compounds present in the flue gas absorb in this spectral range, thus contributing to the total measured absorption. In order to find out how much optical loss can be attributed to broadband processes like SO_2 absorption, a deep ultraviolet LED exhibiting a broad spectral feature around 255 nm was used. As the Hg absorption line is orders of magnitude narrower than the LED peak (*15*), it was shown that the LED intensity is not affected by the presence of Hg^0 in the beam path length. Consequently, the LED signal can be used to remove the part of the Hg lamp intensity loss attributed to all processes except Hg^0 absorption. Ultraviolet light from the Hg lamp and the LED were first combined with a 2×2 fiber coupler. The resulting light was then split into 2 outputs, which exhibited a 9/1 intensity ratio. The weak output was directly connected to a reference channel spectrometer and the strong output was directed across the stack through a collimating lens and a UV transparent window. A receiving lens assembly focused the light transmitted through the stack into a fiber connected to a second spectrometer (measurement channel). Figure 1 depicts the instrumental setup.

The spectrum, consisting of the broad LED feature and the narrow Hg lamp line, was recorded every second on each channel. It was processed in real time by a set of LabVIEW programs which plotted the area under each peak, that is, Hg lamp and LED, versus time. The reference channel, labeled Spec 1 and Laptop 1, monitored optical power drift to correct the signal detected after transmission through the stack by the measurement channel (Spec 2 and Laptop 2). In this way, the intensity fluctuations measured after the stack could be unequivocally attributed to the flue gas.

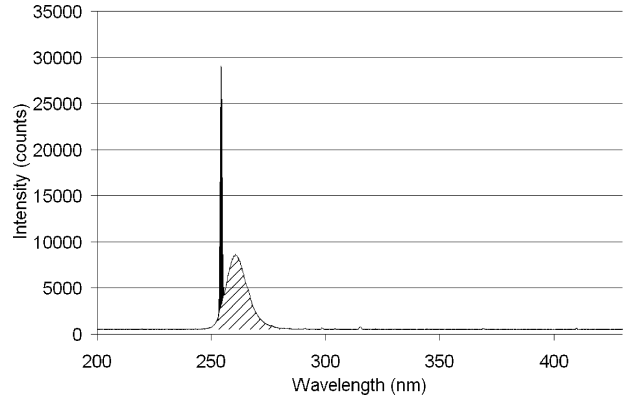

FIGURE 2. Spectrum recorded after mixing the Hg lamp (gray area) and LED (hatched area) emissions.

Figure 2 displays a typical spectrum, the area of the Hg lamp line is highlighted in gray whereas the LED peak is hatched.

A LabVIEW virtual instrument processed the area of each peak continuously. The area values were considered as the measured intensity $I(t)$ of each source, leading to an absorbance value $A(t)$ following the Beer−Lambert relation

$$I(t)/I_0 = \exp(-A(t)) \quad (1)$$

$$A(t) = \alpha(t) \times L = C(t) \times \sigma \times L \quad (2)$$

where $I(t)$ is the area measured in real time, I_0 is the area measured when there is no absorption, $A(t)$ is the absorbance, L is the absorption path length in m and $\alpha(t)$ is the absorption coefficient in m^{-1}. The absorption cross-section, σ, is expressed in accordance with the unit used for the absorbing species concentration, $C(t)$. During this test, $[SO_2]$ was in % so σ_{SO_2} was in m^{-1}, whereas $[Hg^0]$ was in $\mu g/m^3$ leading to σ_{Hg^0} expressed in $m^2/\mu g$.

The setup has been implemented in both laboratory and power plant environments. In the lab, a 0.49 m long absorption cell was used, whereas at the plant, the path length across the stack was 7 m. The main results obtained in the lab and during the field campaign are presented in the following section.

Results and Discussion

Laboratory-Based Work. A temperature-controlled Hg permeation tube was used to supply a stable amount of mercury carried by a nitrogen flow. The stream then passed through a dilution stage, which consisted of the addition of pure nitrogen and/or 0.4% SO_2 in nitrogen, to vary the Hg and SO_2 concentrations before the absorption cell. This configuration allowed for Hg^0 concentrations from 0 to 50 $\mu g/m^3$ and SO_2 concentrations from 0 to 0.18%. Additional details about the experimental apparatus and protocol are available as Supporting Information: refer to section "Supporting Information Available" at the end of this article.

Absorption by SO_2. As a first step, the Hg permeation tube was bypassed to work with SO_2 as the only absorbing species. The SO_2 concentration was gradually increased while recording the intensity, $I(t)$, for both the Hg lamp and the LED. The time chart presented a stair-shape, each step being related to one SO_2 concentration value in the gas stream. Figure 3 shows the linear relation between absorption coefficient α and SO_2 concentration. A different slope value was observed for each source: the absorption cross-section for the LED, σ_{LED}, is 6.64 m^{-1}, which is higher than that of the Hg lamp, $\sigma_{SO_2,Hglamp}$, at 3.92 m^{-1}. These values represent

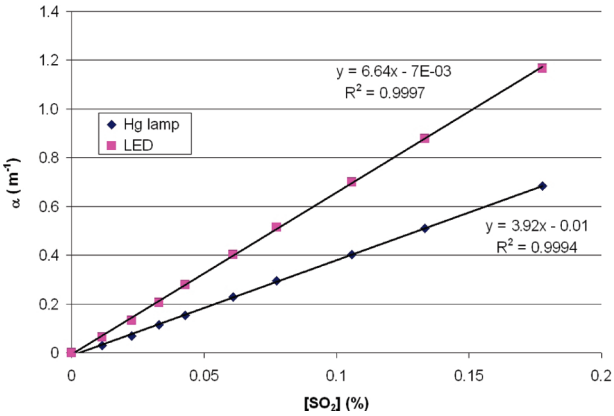

FIGURE 3. Absorption coefficient α versus SO_2 concentration for both Hg lamp and LED.

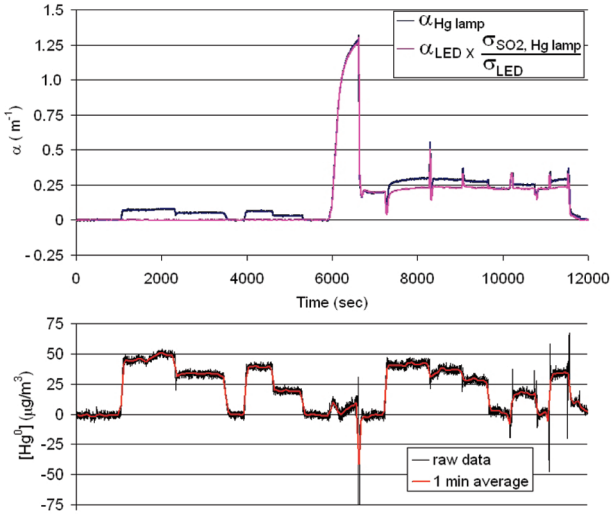

FIGURE 4. Absorption coefficient α versus time (upper chart) and related Hg^0 concentration (lower chart). The LED absorption coefficient, α_{LED}, is scaled by σ_{LED} and $\sigma_{SO_2,Hglamp}$ to get the SO_2 contribution of the Hg lamp absorption coefficient, α_{Hglamp}, as described by eqs 3 and 4.

an important step toward [Hg^0] monitoring in the presence of SO_2: the LED absorption coefficient, α_{LED}, can now be converted into an absolute SO_2 concentration and then into a Hg lamp absorption coefficient, $\alpha_{SO_2,Hglamp}$, as follows:

$$\alpha_{LED}/\sigma_{LED} = [SO_2] \quad (3)$$

$$[SO_2] \times \sigma_{SO_2,Hglamp} = \alpha_{SO_2,Hglamp} \quad (4)$$

Absorption by a Mixture of Hg^0 and SO_2. The second step of this work was to monitor the Hg^0 concentration in the stream with different background concentrations of SO_2. First, the Hg^0 concentration was varied between 0 and 50 $\mu g/m^3$ in pure N_2. Then, a 0.05% SO_2 background was added and the Hg concentration varied between 0 and 45 $\mu g/m^3$. The time chart is presented in Figure 4. The upper graph plots the Hg lamp absorption coefficient, α_{Hglamp}, and the absorption coefficient, $\alpha_{SO_2,Hglamp}$, which is the absorption coefficient, α_{LED}, scaled by σ_{LED} and $\sigma_{SO_2,Hglamp}$ as described by eqs 3 and 4. In this way, $\alpha_{SO_2,Hglamp}$ represents the SO_2 contribution of the Hg lamp absorption, and it can be subtracted to yield the Hg^0 absorption only

$$\alpha_{Hglamp} - \alpha_{SO_2,Hglamp} = \alpha_{Hg^0,Hglamp} \quad (5)$$

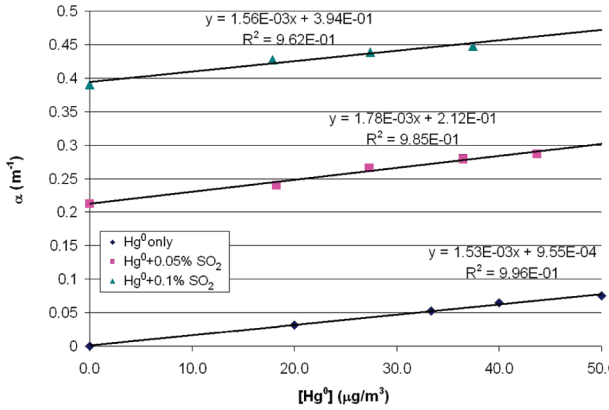

FIGURE 5. Absorption coefficient, α, versus [Hg^0] for different SO_2 settings.

Eventually, the remaining absorption coefficient, $\alpha_{Hg^0,Hglamp}$, leads to Hg^0 concentration as follows:

$$\alpha_{Hg^0,Hglamp}/\sigma_{Hg^0,Hglamp} = [Hg^0] \quad (6)$$

Until $t = 6000$ s, the LED signal remained null because no SO_2 was present in the stream. At $t = 6000$ s, a sudden and large intake of SO_2 in the absence of Hg^0 caused a large increase of both Hg lamp and LED absorption coefficients. After this point, the Hg^0 concentration was varied while the SO_2 concentration was kept at 0.05%.

The lower chart demonstrates that the Hg^0 concentration can be determined even in the presence of SO_2 thanks to the LED background correction. However, some concentration spikes are noticeable at points when the gas mixture composition was rapidly modified in the absorption cell. Indeed, the high acquisition rate (one concentration point per second) allows the system to capture the transient composition of the gas mixture. However, the cross-section of the ultraviolet beam, which consists in a Hg lamp component and an LED component, is not spatially homogeneous. As a consequence, when a transverse concentration gradient appears in the volume probed by the beam (i.e., in the absorption cell), the LED signal does not accurately correct the Hg lamp signal and concentration spikes occur. Once the gas mixture is homogeneous, the correction procedure works properly and the Hg^0 concentration becomes accurate. This problem was faced in the lab because the fast flow rate changes required a couple of seconds to let the gas mixture become homogeneous. It is very unlikely that this issue will appear during field measurements because the volume probed by the ultraviolet beam is very small compared to the total volume of the gaseous exhaust of a power plant and, consequently, the flue gas composition can be considered homogeneous within the transverse plane of the ultraviolet beam.

Finally, the same test was repeated with 0.1% SO_2. Figure 5 shows the absorption coefficient, α, plotted versus Hg^0 concentration for the three different SO_2 backgrounds. One can notice a very good linearity between α and [Hg^0] for the three data series and the slope value remains independent of the SO_2 concentration. This is a crucial point because it means the linear relation between the response of the sensor and [Hg^0] is independent of the SO_2 background concentration. The *y*-intercept value, α_0, for the 0.05% SO_2 setting is 0.21 m^{-1}, which compares well to the expected value from the measured $\sigma_{SO_2,Hglamp}$ (see Figure 3), $\alpha_0 = \sigma_{SO_2,Hglamp} \times [SO_2] = 3.92 \times 0.05 = 0.20\ m^{-1}$. In the same way, $\alpha_0 = 0.39\ m^{-1}$ for the 0.1% SO_2 experiment, and the expected value is $\alpha_0 = 3.92 \times 0.1 = 0.39\ m^{-1}$. This excellent agreement shows that the absorption cross-section that was measured with SO_2 only, $\sigma_{SO_2,Hglamp}$, allows one to convert an absorbance

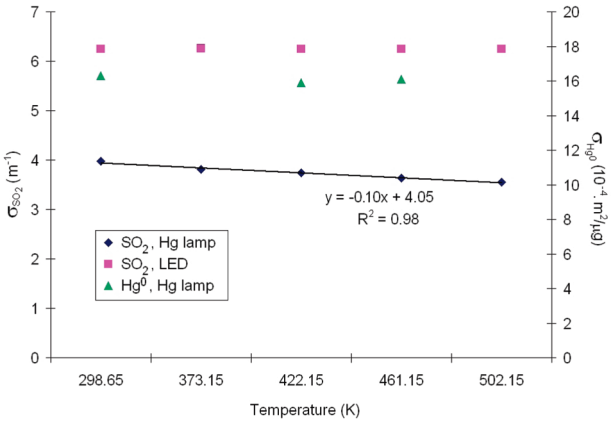

FIGURE 6. Temperature dependence of the SO_2 absorption cross sections, $\sigma_{SO_2,LED}$ and $\sigma_{SO_2,Hglamp}$, for the LED and the Hg lamp measurements respectively, as well as the Hg^0 absorption cross-section, $\sigma_{Hg^0,Hglamp}$, for the Hg lamp.

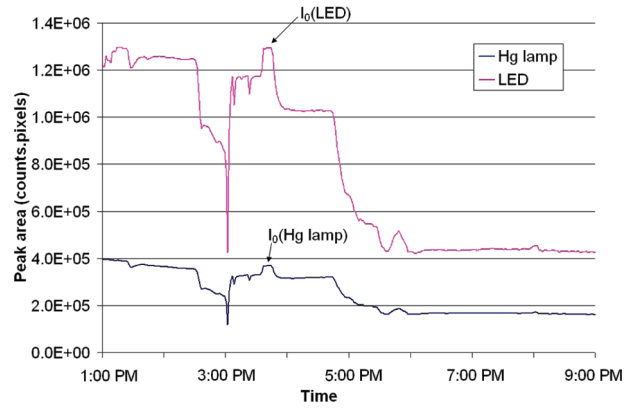

FIGURE 7. Transmission versus time during the burner start-up.

measured in the presence of Hg^0 into an absolute SO_2 concentration. The average of the three slope values ($\pm 2\sigma$) gives $\sigma_{Hg^0,Hglamp} = (1.62 \pm 0.27) \times 10^{-3}$ m^2/μg.

Absorption Cross-Section Temperature Dependence. Since the flue gas temperature is expected to be between 180 and 200 °C, the method's sensitivity to temperature was investigated. This was accomplished by placing the absorption cell into a cylindrical temperature-controlled furnace: the temperature was varied between 25 and 230 °C and, for each temperature step, the absorption coefficient, α, was plotted versus the concentration to get the absorption cross-section, σ, provided by the slope of the linear fit.

Figure 6 shows the evolution of the absorption cross sections when the gas stream temperature was varied from 25 to 230 °C. At first, the SO_2 absorption cross-section was investigated alone by plotting the absorption coefficient of the Hg lamp, α_{Hglamp}, and the LED, α_{LED}, versus the SO_2 concentration, as illustrated in Figure 3, at 25, 100, 150, 180, and 230 °C. No significant temperature dependence was found for the LED absorption cross-section, $\sigma_{SO_2,LED}$, whereas a linear decrease of 11% of the $\sigma_{SO_2,Hglamp}$ value was observed between 25 and 230 °C. When temperature increases, peak cross sections of vibrational bands decrease while the line widths and band contours of the absorption features become broader (*16*). Since the LED emission is broad compared to the vibrational band peaks, its absorption by SO_2 is not affected by the temperature induced broadening. Conversely, the narrow emission of the Hg lamp at 253.7 nm is altered by the SO_2 absorption cross-section decrease at this specific wavelength. This temperature dependence will have to be accounted for in hot flue gas measurements.

The same test was then performed with a pure stream of elemental mercury diluted in nitrogen at 25, 150, and 180 °C. Because the upper energy state of the mercury transition is relatively high ($E(6^3P_1) = 39412.300$ cm^{-1} (*17*)), the population change between 25 and 180 °C is negligible, according to the Boltzmann distribution. Indeed, no significant change of $\sigma_{Hg^0,Hglamp}$ was measured within this temperature range, as depicted in Figure 6.

Detection Limit Evaluation. During these experiments, the noise-equivalent concentration, NEC, was measured being NEC = STDEV × 3 = 1.6 × 3 = 4.9 μg/m^3 (assuming that the noise is randomly distributed and that it follows the normal law, 99.7% of the data lie within three standard deviations). Considering a minimum detectable concentration for a signal-to-noise ratio of 3, we get $[Hg^0]_{min} = 14.7$ μg/m^3 for an absorption path length of 49 cm and an acquisition frequency of 1 spectrum per second. Figure 4 (lower chart) shows that averaging over 1 min ($N = 60$ data points) improves drastically the signal-to-noise ratio, and the minimum detectable concentration becomes $[Hg^0]_{min}/(N)^{1/2} = 1.9$ μg/m^3. If increasing the absorption path length decreases the limit of detection linearly, a path length of 7 m would lead to a minimum detectable concentration better than 0.2 μg/m^3 at the power station.

Field Campaign at 230 MW Coal-Fired Power Plant. As the laboratory work showed the feasibility of in situ Hg^0 trace monitoring in the presence of SO_2, the sensor was taken to a 230 MW power plant in order to assess its operation in the field. The instrument was installed at a level approximately half way up the 75 m tall stack, where a platform is dedicated to stack analyzers. As shown in Figure 1, the UV beam crossed the stack diameter to probe in situ Hg^0 and SO_2 in the flue gas. The sensor was located after the electrostatic precipitator, and the flow was thus relatively free of particulate matter as indicated by the opacimeter running at the same level in the stack.

Figure 7 presents the measurements performed at the beginning of the trial. This period was crucial since the stack exhaust was probed during the start-up of the burners. From 1:00 p.m. to 3:45 p.m., the station was shut down, and thus no combustion exhaust was released. A clean air stream flushed the stack for half an hour (2:30 to 3:00 p.m.) in order to remove any remaining absorbing species. After preliminary optical adjustments, the reference level, I_0 (the signal with no absorption), was observed for both the Hg lamp and the LED as pointed out in Figure 7.

At 3:45 p.m., a one hour burner warm-up period began, during which time the boiler was supplied with natural gas. During this period, both Hg lamp and LED signals displayed a rapid drop followed by a plateau, indicating that part of the light was absorbed by the flue gas. At 4:45 p.m., the station switched to regular coal settings to run overnight. The transmitted intensity dropped again for both Hg lamp and LED before reaching a plateau.

Owing to the calibration work carried out at the lab, the LED absorption can be converted into an SO_2 concentration according to eq 3. The result is displayed in Figure 8 (solid line). The 15 min averaged SO_2 measurements performed by the analyzer at the same level in the stack are also plotted for comparison (the lack of data around 5 p.m. is caused by an automated calibration of the instrument at a concentration of 350 ppm). A good agreement is observed between the data from the in situ absorption CEM and the extractive instrument. Therefore, the absorption cross-section, σ_{LED}, determined in the lab allowed an accurate conversion of the absorption coefficient, α_{LED}, into concentration of SO_2 in the power plant exhaust. It also confirmed that SO_2 absorption was the only broadband loss process in the flue gas at 254 nm. In other words, neither scattering, nor additional absorption from species such as NO_2 were measured during the test, as monitored by the analyzers running in the stack.

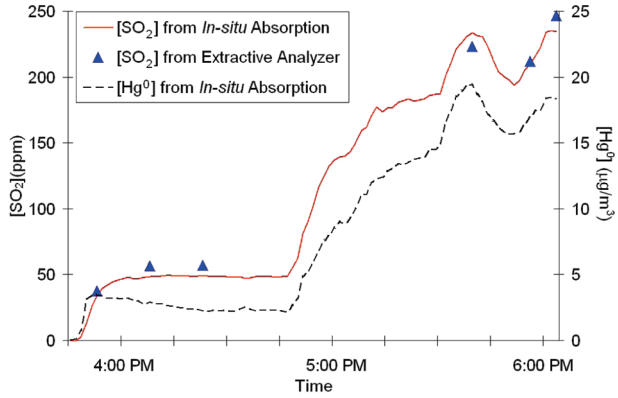

FIGURE 8. SO_2 and Hg^0 concentrations versus time during the burner start-up. NB: The lack of data from the SO_2 analyzer around 5 p.m. was because of its automated calibration routine over that period.

Once the SO_2 concentration is known, eq 4 allows one to solve for $\alpha_{SO_2,Hglamp}$, the part of the total Hg lamp absorption coefficient, α_{Hglamp}, attributed to SO_2. This value can thus be removed to get $\alpha_{Hg^0,Hglamp}$, the part of the signal attributed to Hg^0 as described by eq 5. Finally, the absolute concentration, $[Hg^0]$, is determined using $\sigma_{Hg^0,Hglamp}$ (see eq 6), which was determined in the lab. The resulting signal is displayed by the dashed line in Figure 8.

Unlike SO_2, no mercury measurement was performed by an accepted standard method during the test. As a consequence, the Hg^0 concentration provided by the in situ CEM could not be compared and validated. However, the Hg^0 concentration was found in the expected range of 1−30 $\mu g/m^3$ (*9*, *10*). Qualitatively, a correlation was observed between SO_2 and Hg^0. This can simply be explained as equivalent variations in both species' concentrations resulting from fluctuations in the temperature and pressure within the stack. These fluctuations arise from changes upstream, such as starting up the burners at 3:45 p.m. and switching to coal combustion at 4:45 p.m. Further insvestigation is necessary to identify the cause of this correlation as it could only be a function of plant operations and controls.

After a few hours, the transmission through the stack decreased slowly, independently of the flue gas content. This loss was attributed to the UV transparent windows which appeared slightly contaminated. As a consequence, SO_2 absorption was not the only ultraviolet broadband loss anymore and the UV beam attenuation had an unquantified contribution from the windows' opacity. The attenuation background could not be removed accurately anymore from the Hg lamp signal at 253.7 nm, causing the sensor to provide inaccurate SO_2 and Hg^0 concentration values. The actual version of the in situ CEM requires that the attenuation background around 254 nm is only because of SO_2 absorption. To verify that condition, an SO_2 analyzer must provide an independent measurement for comparison purpose. As long as the SO_2 concentrations from the in situ CEM and the analyzer compare well (as it was the case during the start-up of the power plant), it can be concluded that SO_2 absorption is the only broadband loss process and Hg^0 can be determined as it was established by the prior laboratory tests.

The goal of this early field trial was to run the sensor in a full scale power plant in order to make a first assessment of its operation and orientate future development efforts. First of all, this test showed that the instrumental setup was operable in an industrial environment. Its simple optical lay-out, combined with fibered light sources and spectrometers, led to a rugged system and a quick installation (around 2 h, optical alignment included). Then, in situ absorption data were collected in the stack of the plant for the first time, resulting in SO_2 and Hg^0 concentration values during the start-up of the plant. However, the transmission loss of the optical windows after a few hours of operation evidenced the need of upgraded flanges equipped with air jets keeping the windows clean on a longer term basis. Finally, the Hg^0 concentration could not be certified because of the absence of comparison with independent Hg concentration measurements. A new field trial involving simultaneous mercury measurements by an accepted standard method will be the next step to assess the accuracy and uncertainty of the elemental mercury in situ CEM measurements.

Acknowledgments

The authors thank Ontario Centres of Excellence for funding this work and Mr. Brian Bowles from Resonance Ltd. for building power supply electronics for the LED. A patent application, entitled "Apparatus for Continuous In Situ Monitoring of Elemental Mercury Vapour, and Method of Using Same", has been filed for this instrument.

Supporting Information Available

More details about the experimental apparatus and protocol. This information is available free of charge via the Internet at http://pubs.acs.org.

Literature Cited

(1) Ullrich, S. M.; Tanton, T. W.; Abdrashitova, S. A. Mercury in the Aquatic Environment: A Review of Factors Affecting Methylation. *Crit. Rev. Environ. Sci. Technol.* **2001**, *31*, 241–293.
(2) *Canada-Wide Standards For Mercury Emissions From Coal-Fired Electric Power Generation Plants*; Canadian Council of Ministers of the Environment: Quebec City, Canada, 2006.
(3) *Long-Term Field Evaluation of Mercury (Hg) Continuous Emission Monitoring Systems*; United States Environmental Protection Agency: Washington, DC, 2006.
(4) Srivastava, R.; Hutson, N.; Martin, B.; Princiotta, F.; Staudt, J. Control of mercury emissions from coal-fired electric utility boilers. *Environ. Sci. Technol.* **2006**, *40*, 1385–1393.
(5) Graydon, J. W.; Zhang, X.; Kirk, D. W.; Jia, C. Q. Sorption and stability of mercury on activated carbon for emission control. *J. Hazard. Mater.* **2009**, *168*, 978–982.
(6) Laudal, D. L.; Thompson, J. S.; Pavlish, J. H.; Brickett, L. A.; Chu, P. Use of continuous mercury monitors at coal-fired utilities. *Fuel Process. Technol.* **2004**, *85*, 501–511.
(7) Gleason, R. L.; Hahn, D. W. The effects of oxygen on the detection of mercury using laser-induced breakdown spectroscopy. *Spectrochim. Acta, Part B* **2001**, *56*, 419–430.
(8) Buckley, S. G.; Johnsen, H. A.; Hencken, K. R.; Hahn, D. W. Implementation of laser-induced breakdown spectroscopy as a continuous emissions monitor for toxic metals. *Waste Manage.* **2000**, *20*, 455–462.
(9) Evans, A.; Redinger, K.; Holmes, M. Advanced Emissions Control Development Program: Mercury Control. Presented at the Advanced Coal-Based Power and Environmental Systems Conference, 1997.
(10) *Measurements of Speciated Mercury Emissions from Ontario Generating Stations*; Ontario Hydro Technologies: Ontario, Canada, 1999.
(11) Senior, C. L. Behavior of Mercury in Air Pollution Control Devices on Coal-Fired Utility Boilers. *Power Production in the 21st Century: Impacts of Fuel Quality and Operations*, Engineering Foundation Conference, Snowbird, UT, October 28−November 2, 2001.
(12) Yan, N.-Q.; Qu, Z.; Chi, Y.; Qiao, S.-H.; Dod, R. L.; Chang, S.-G.; Miller, C. Enhanced Elemental Mercury Removal from Coal-Fired Flue Gas by Sulfur-Chlorine Compounds. *Environ. Sci. Technol.* **2009**, *43*, 5410–5415.
(13) Anderson, T.; Magnuson, J.; Lucht, R. Diode-laser-based sensor for ultraviolet absorption measurements of atomic mercury. *Appl. Phys. B: Lasers Opt.* **2007**, *87*, 341–353.
(14) Hoops, A. A.; Farrow, R. L.; Schulz, P.; Reichardt, T. A.; Bambha, R. P.; Schmitt, R. L.; Kliner, D. A. V. Compact, narrow-linewidth, tunable ultraviolet laser source for detecting Hg emissions. *Proc. SPIE* **2008**, *6875*, 68750K.

(15) Turgeon, E. C.; Shepherd, G. G. Upper atmospheric temperatures from Doppler line widths-II: Measurements on the OI 5577 and OI 6300 lines in aurora. *Planet. Space Sci.* **1962**, *9*, 295–304.
(16) Wu, C. Y. R.; Yang, B. W.; Chen, F. Z.; Judge, D. L.; Caldwell, J.; Trafton, L. M. Measurements of High-, Room-, and Low-Temperature Photoabsorption Cross Sections of SO_2 in the 2080- to 2950- Region, with Application to Io. *Icarus* **2000**, *145*, 289–296.
(17) Basic Atomic Spectroscopic Data from NIST. http://physics.nist.gov/PhysRefData/Handbook/Tables/mercurytable5.htm (accessed 2009).

ES902409T